Eur J Appl Physiol (2014) 114:165–175
DOI 10.1007/s00421-013-2754-0

ORIGINAL ARTICLE

A mathematical model for carbon dioxide elimination: an insight for tuning mechanical ventilation

Anake Pomprapa · David Schwaiberger · Burkhard Lachmann · Steffen Leonhardt

Received: 18 July 2013 / Accepted: 10 October 2013 / Published online: 27 October 2013

Abstract
Purpose The aim is to provide better understanding of carbon dioxide (CO_2) elimination during ventilation for both the healthy and atelectatic condition, derived in a pressure-controlled mode. Therefore, we present a theoretical analysis of CO_2 elimination of healthy and diseased lungs.
Methods Based on a single-compartment model, CO_2 elimination is mathematically modeled and its contours were plotted as a function of temporal settings and driving pressure. The model was validated within some level of tolerance on an average of 4.9 % using porcine dynamics.
Results CO_2 elimination is affected by various factors, including driving pressure, temporal variables from mechanical ventilator settings, lung mechanics and metabolic rate.
Conclusion During respiratory care, CO_2 elimination is a key parameter for bedside monitoring, especially for patients with pulmonary disease. This parameter provides valuable insight into the status of an atelectatic lung and of cardiopulmonary pathophysiology. Therefore, control of CO_2 elimination should be based on the fine tuning of the driving pressure and temporal ventilator settings. However, for critical condition of hypercapnia, airway resistance during inspiration and expiration should be additionally measured to determine the optimal percent inspiratory time (%TI) to maximize CO_2 elimination for treating patients with hypercapnia.

Keywords CO_2 elimination · Volumetric capnogram · Tidal volume model · AutoPEEP model · ARDS

Communicated by David C. Poole.

A. Pomprapa and D. Schwaiberger contributed equally to this work.

A. Pomprapa (✉) · S. Leonhardt
Philips Chair for Medical Information Technology, Helmholtz-Institute for Biomedical Engineering, RWTH Aachen University, Aachen 52074, Germany
e-mail: pomprapa@hia.rwth-aachen.de

D. Schwaiberger · B. Lachmann
Department of Anesthesiology and Intensive Care Medicine, Campus Virchow Klinikum, Charité University Hospital Berlin, Berlin 13353, Germany

Introduction

Acute respiratory distress syndrome (ARDS) is characterized by dysfunction of the alveoli-capillary unit. Activation of inflammatory mediators leads to protein-rich edema and surfactant dysfunction, which results in development of atelectasis with right-to-left pulmonary shunt leading to hypercapnia and hypoxia. At the same time, remodeling of damaged lung tissue starts, which also leads to a rise in pulmonary arterial pressure and a decrease in pulmonary compliance.

Treatment of ARDS is mainly based on lung-protective ventilation. Various ventilation techniques can be employed; for instance, application of a high positive end-expiratory pressure (PEEP) to prevent collapse of alveoli at the end of expiration and to improve oxygenation (Ashbaugh et al. 1967), high-frequency ventilation (Krishnan and Brower 2000), or the ARDSnet protocol with low tidal volume to reduce mortality rate compared with conventional ventilation (NHLBI 2000).

One side-effect of ventilation with low tidal volumes is possible retention of CO_2. Although this 'permissive hypercapnia' is a common approach in the treatment of

ARDS (Amato et al. 1998), higher levels of $PaCO_2$ can lead to respiratory acidosis with deleterious effects on hemodynamic stability (Thorens et al. 1996; Beitler et al. 2013). Massive hypercapnia can lead to severe organ dysfunction (Hickling and Joyce 1995). Most important, hypercapnia increases intracranial pressure (Marx et al. 1973), which leads to an impairment of cerebral perfusion pressure and can augment risk for cerebrovascular complications. Additionally, hypercapnia increases pulmonary vasoconstriction (Dorrington and Talbot 2004), which leads to right heart failure (Mekontso et al. 2009) due to pulmonary hypertension. Furthermore, there is an evidence that hypercapnia has adverse effects on the developing retina in children (Bauer 1982).

Therefore, effective elimination of CO_2 should be another goal in the treatment of ARDS. CO_2 is typically produced by cell metabolism and dissolves in blood circulation. During ventilation, blood with a high CO_2 concentration is transported to the lung for gas exchange and CO_2 is eliminated during expiration. The flow of CO_2 exhaled in ml/min is referred to as CO_2 elimination and CO_2 can be only removed by the ventilation process. The respiratory settings, which affect CO_2 elimination, are respiratory rate (RR), inspiratory time, peak inspiratory pressure (PIP) and PEEP.

From a historical perspective, CO_2 elimination started to be investigated after methods and means for breath-by-breath analysis became available (Lipsky and Angelone 1967). Slutsky et al. (1981) reported that CO_2 elimination increased monotonically with RR at constant tidal volume (V_T) and the model prediction for CO_2 elimination based on paralyzed dogs depended on a nonlinear relationship between RR and V_T($\dot{V}_{CO_2} = k \cdot RR^a \cdot V_T^b$, k, a and c are constants obtained by multiple regression).

Lachmann et al. (1989) examined and reported that CO_2 elimination could be improved by adapting the I:E ratio in patients with ARDS. For anesthetized children, Lindahl et al. (1989) computed CO_2 elimination based on a weight basis, which is $\dot{V}_{CO_2} = -1.25 \cdot X + 13 \cdot X^2$, where $X = \log_e$ (bodyweight, kg).

Larsson (1992) suggested that CO_2 elimination can be improved by minimization of apparatus dead space. In 1994, Saidel and Chang (1994) showed that $PaCO_2$ can be expressed in terms of first-order linear differential equation with exogenous input of metabolic rate. For clinical application, this implies that CO_2 elimination should be adjusted to cope with the metabolic rate for ventilation at steady state.

Taskar et al. (1995) examined the dynamics of CO_2 elimination after ventilation resetting in forty-four patients. They found that the relative change in CO_2 elimination was proportional to the relative change in V_T. Breen and Mazumdar (1996) investigated the effect of PEEP on CO_2 elimination and showed that high PEEP increases anatomical dead space in anesthetized dogs and decreases pulmonary CO_2 elimination per breath. Similar results were confirmed by Tusman et al. (2010) in anesthetized pigs.

Devaquet et al. (2008) found that a postinspiratory pause has a significant influence on CO_2 elimination for patients with acute lung injury (ALI). A recent study (Aboab et al. 2012) pointed out that an inspiratory flow pattern with long mean distribution time and high end-inspiratory flow enhances CO_2 elimination. CO_2 elimination can be used not only for the treatment of hypercapnia, but also for the assessment of pulmonary perfusion (Fletcher 1986).

In summary, the previous contributions of CO_2 elimination were mainly associated with scientific findings or the techniques of ventilation for enhancing CO_2 elimination. Minimal mathematical models for CO_2 elimination were introduced.

The aim of this work is, therefore, to introduce a mathematical model of CO_2 elimination based on ventilation variables for application in patients with ARDS to evaluate CO_2 removal.

Materials and methods

Hardware configuration

The open-loop system consists of a medical guide Panel PC for data collection (PPC-154T, Advantech Co., Ltd, Taipei, Taiwan), a mechanical ventilator (EVITA XL, Draeger AG, Luebeck, Germany) and several measuring devices including a spectrophotometer (CeVOX, Pulsion Medical Systems SE, Munich, Germany) to measure arterial oxygen saturation (SaO_2), a hemodynamic monitor (Sirecust 960, Siemens AG, Munich, Germany), and an integrated sensor called Capno Plus (Option for EVITA XL, Draeger AG, Luebeck, Germany), which is used to measure CO_2 for further computation of breath-by-breath CO_2 elimination.

Data on airway flow and percentage of CO_2 concentration are transferred from the ventilator to the Panel PC by a serial Medibus connection. The computation is carried out with a sampling time of 8 ms for monitoring of breath-by-breath CO_2 elimination. CO_2 elimination is computed by Eq. (1) (Breen et al. 1992) during expiration using Labview software (Version 7.1, National Instruments).

$$\dot{V}_{CO_2} = \frac{RR}{60} \times \int_{T_{in}}^{T_{in}+T_{ex}} \dot{V}(t) \times \frac{[CO_2(t)]}{100} dt \quad (1)$$

where $\dot{V}_{CO_2}$ is the CO_2 elimination (ml/min), RR is the respiratory rate (bpm), $\dot{V}(t)$ is the airway flow (ml/min), $[CO_2(t)]$ is the measured percent of carbon dioxide

concentration (%), T_{in} is the inspiratory time (s) and T_{ex} is the expiratory time (s).

Single-compartment modeling

The respiratory system is simplified using a single-compartment model (Marini et al. 1989; Leonhardt et al. 1998) associated with an electrical circuit (Fig. 1). This simple model provides a practical solution for routine clinical application with no need for additional sensors inserted in the lung compartments. The model assumes normal ventilation, with no hysteresis, and no opening and closing of airspace in the lung during the respiratory cycle. The model variables are defined as follows.

Airway resistances (R_{in} and R_{ex}) represent the friction coefficient of air flow characterizing the endotracheal tube, trachea, bronchi and bronchioles. For bronchioles, millions of alveolar sacs are modeled as one capacitor (C_{rs}) characterizing the capacity of lung volume storage in lung mechanics.

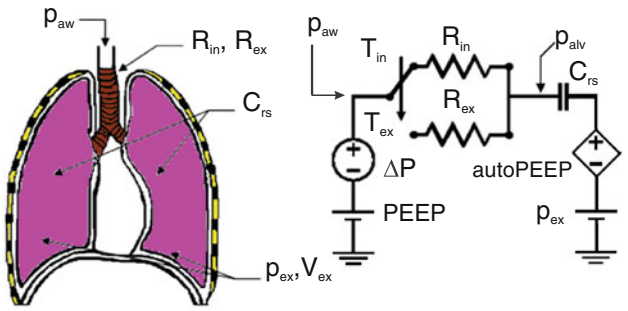

Fig. 1 Simplified electrical circuit analogous to lung mechanics

Additionally, a positive alveolar pressure at end-expiration (so-called autoPEEP) is incorporated in the model. Thus, autoPEEP is the pressure remaining in the lung at end-expiration, caused by gas held in the alveoli (Mughal et al. 2005).

p_{aw} denotes the airway pressure applied to the subject in a pressure-controlled mode. The airway pressure (p_{aw}) is considered to have a driving pressure ΔP during inspiratory time (T_{in}) and zero mbar during expiratory time (T_{ex}). In the model, a switching element is used to separate the two resistance components (R_{in} and R_{ex}) for inspiration and expiration, respectively.

The RR is equivalent to $\frac{60}{T_{in}+T_{ex}}$, percent inspiratory time (%TI) is defined as $\frac{100\times T_{in}}{T_{in}+T_{ex}}$ and C_{rs} denotes lung compliance:

$$C_{rs} = \frac{V_T}{\Delta P - \text{autoPEEP}(T_{ex})} \tag{2}$$

where V_T represents tidal volume and autoPEEP is a function of expiratory time (T_{ex}) or RR and %TI. Applying Kirchhoff's voltage law in the circuit model during respiration, this yields Eqs. (3) and (4) for $\dot{V} > 0$ and $\dot{V} < 0$ corresponding to inspiration and expiration, respectively.

$$p_{aw}(t) = R_{in} \times \dot{V}(t) + \frac{V(t)}{C_{rs}} + \text{autoPEEP}(T_{ex}) \tag{3}$$

$$p_{aw}(t) = R_{ex} \times \dot{V}(t) + \frac{V(t)}{C_{rs}} + \text{autoPEEP}(T_{ex}) \tag{4}$$

C_{rs}, R_{in} and R_{ex} are assumed to be constant and the specified inspired tidal volume can be solved using the Laplace transform with an initial condition $V_i(0) = 0$. An ideal curve of pressure-controlled ventilation is shown in Fig. 2.

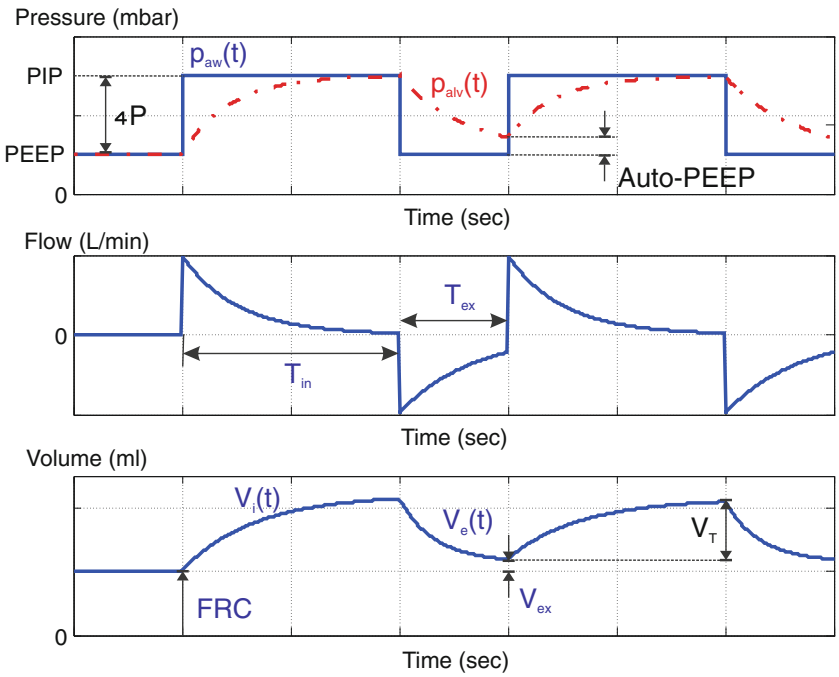

Fig. 2 Ideal curve of pressure-controlled ventilation for a single-compartment lung

Note that due to the pressure dependency of alveolar opening and closing, the functional residual capacity [FRC(PEEP)] (Webster 2009) is a function of PEEP itself. AutoPEEP causes an end-expiratory volume (V_{ex}), which is an additional volume above the underlying FRC. Therefore, the maximum lung volume during the tidal cycle can be expressed as

$$V_{max} = \text{FRC} + V_{ex} + V_T \quad (5)$$

Equation (5) implies that lung volume is fixed to a certain value during ventilation in pressure-controlled mode. The total PEEP (PEEP_T) corresponds to the alveolar pressure at the end of expiration and can be expressed as

$$\text{PEEP}_T = \text{PEEP} + \text{autoPEEP}(\text{RR}, \%\text{TI}) \quad (6)$$

To compute V_T, Eqs. (3) and (4) allow estimation of tidal volume; mathematical proof is presented in the "Appendix I". Tidal volume can be solved as provided in Eq. (7), which is a nonlinear function of the ventilation settings and lung mechanics parameters.

$$\tilde{V}_T = C_{rs}\Delta P \times \frac{\left(1 - e^{\frac{-60\times\%\text{TI}/100}{R_{in}C_{rs}\times\text{RR}}}\right) \times \left(1 - e^{\frac{-60\times(1-\%\text{TI}/100)}{R_{ex}C_{rs}\times\text{RR}}}\right)}{1 - e^{\frac{-60\times\%\text{TI}/100}{R_{in}C_{rs}\times RR}} \times e^{\frac{-60\times(1-\%\text{TI}/100)}{R_{ex}C_{rs}\times\text{RR}}}} \quad (7)$$

The parameters RR and %TI are two independent temporal variables to shape tidal volume. They are incorporated with the lung mechanics parameters, forming a nonlinear exponential function as a correcting factor to $C_{rs}\Delta P$. Tidal volume can be estimated using this mathematical model.

Estimation of airway dead space

Airway dead space (V_D) is the volume of conducting airway that does not participate in gas exchange consisting of trachea to the bronchioles. Fletcher and Jonson (1984) divided the response of CO_2 from the volumetric capnogram into three distinct phases (Fig. 3). Phase I represents carbon dioxide-free expiration, i.e., there is no CO_2 concentration during expiration. Phase II appears as an S-shape increasing upwards, which is the mixing phase of the terminal gas between the conducting airways and alveolar gas. Phase III is the 'alveolar plateau' representing gas from the alveoli (Girard and Bernard 2007).

The dead space ratio ($\tilde{V}_D/V_T$) can be estimated from the concept of efficiency (Sinha et al. 2011; Fletcher et al. 1981), derived from the volumetric capnogram (Fig. 3). This method is closely related to Bohr's concept, which is practical for clinical use. The shaded area quantified with X is the volume of CO_2 gathering in dead space from a single breath, and the area ABCDA hypothetically describes the effective volume of gas that can be eliminated in a single breath.

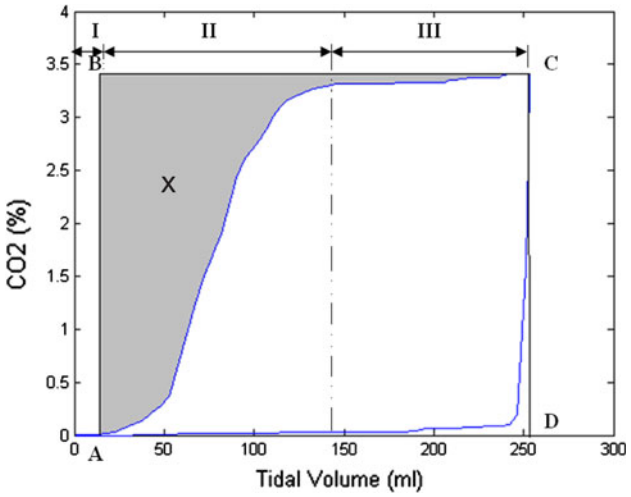

Fig. 3 Volumetric capnogram from single-breath CO_2 analysis from an animal experiment

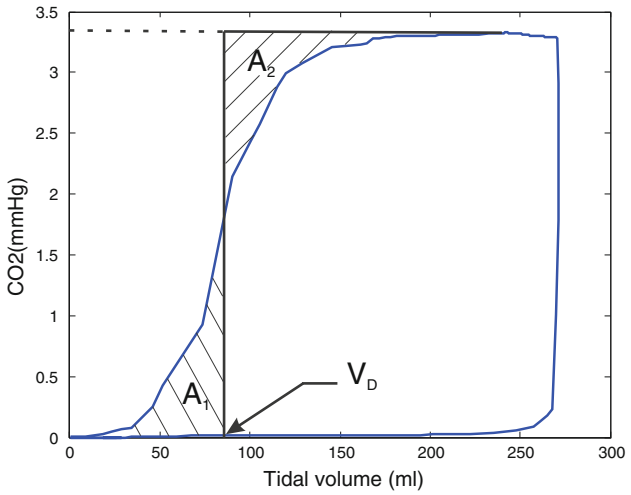

Fig. 4 Volumetric capnogram for estimation of CO_2 elimination

$$\tilde{V}_D = \frac{X}{\text{ABCDA}} \times V_T. \quad (8)$$

Mathematical model of CO_2 elimination

In Fig. 4, the airway dead space lies at a certain point in Phase II and is represented by V_D. A_1 is the amount of exhaled CO_2 (in ml) obtained from the dead space. When the amount of CO_2 from A_1 is theoretically mapped to A_2, the perfect pulse of CO_2 can be obtained with a delay caused by airway dead space. With this concept, the amount of CO_2 during expiration can be computed by multiplying end-tidal CO_2 in percent ($[\text{etCO}_2]$) and the volume difference between tidal volume and airway dead space.

Minute alveolar ventilation ($\dot{V}_A$) (ml/min) can be estimated from Eq. (9), where $\tilde{V}_D$ denotes the estimated dead

space obtained from the volumetric capnogram. The difference between tidal volume and airway dead space corresponds to the air volume in the alveoli involved in gas exchange.

$$\dot{V}_{\mathrm{A}} = \mathrm{RR} \times (V_{\mathrm{T}} - \tilde{V}_{\mathrm{D}}) \tag{9}$$

CO_2 elimination ($\dot{V}_{CO_2}$) can also be estimated by multiplying $[\mathrm{etCO_2}]/100$ by the minute alveolar ventilation provided in Eq. (10).

$$\tilde{\dot{V}}_{\mathrm{CO_2}} = \frac{[et\mathrm{CO_2}]}{100} \times \dot{V}_{\mathrm{A}} \tag{10}$$

Substituting Eq. (7) into Eq. (8) and Eq. (9) into Eq. (10), CO_2 elimination proves to be a nonlinear function depending on the percent of $etCO_2$ during expiration, and on the various lung mechanics parameters and on ventilation settings.

$$\tilde{\dot{V}}_{\mathrm{CO_2}} = \frac{[et\mathrm{CO_2}]}{100} \times \mathrm{RR} \times \left\{ C_{\mathrm{rs}} \Delta P \times \frac{\left(1 - e^{\frac{-60 \times \%\mathrm{TI}/100}{R_{\mathrm{in}} C_{\mathrm{rs}} \times \mathrm{RR}}}\right) \times \left(1 - e^{\frac{-60 \times (1 - \%\mathrm{TI}/100)}{R_{\mathrm{ex}} C_{\mathrm{rs}} \times \mathrm{RR}}}\right)}{1 - e^{\frac{-60 \times \%\mathrm{TI}/100}{R_{\mathrm{in}} C_{\mathrm{rs}} \times \mathrm{RR}}} \times e^{\frac{-60 \times (1 - \%\mathrm{TI}/100)}{R_{\mathrm{ex}} C_{\mathrm{rs}} \times \mathrm{RR}}}} - \tilde{V}_{\mathrm{D}} \right\} \tag{11}$$

We can see from Eq. (11) that the ventilatory variables (ΔP, RR and %TI) result in a change of CO_2 elimination, as shown in Fig. 5.

The simulation results based on a change of these ventilatory variables are presented in Figs. 9 and 10, derived from a pig with different pathophysiology (a healthy and an induced ARDS condition). We can also extend Eq. (11) for volume-controlled ventilation by replacing the estimation of tidal volume from Eq. (7) by the setting volume. Therefore, computation of CO_2 elimination can be made for volume-controlled ventilation based on Eq. (11).

Experiment protocol

After approval from the local animal ethics committee, two female domestic pigs (33 and 35 kg) were premedicated and received adequate anesthesia before the experiment. The premedication was introduced to the subject with ketamine, xylazine and azaperone by intramuscular injection into the neck muscle. After 30 min, anesthesia was introduced with propofol (2–4 mg/kg), fentanyl (0.01–0.02 mg/kg) and pancuronium (0.2 mg/kg). The anesthesia was maintained with thiopental (14–20 mg/kg/h), fentanyl (2–6 g/kg/h) and pancuronium (0.1 mg/kg). The pigs were subsequently tracheotomized and ventilated in supine position. A catheter for SaO_2 measurement was placed in the carotid artery. The ventilator was set to the airway pressure release ventilation (APRV) mode and various ventilation settings (including RR, %TI, PEEP and PIP) were manually adjusted to collect data on CO_2 elimination. Lung injury was induced in the second (35 kg) pig by lung lavage with 0.9 % warmed saline solution (Lachmann et al. 1980). PEEP and PIP were set so that tidal volume ranged from 3 to 10 ml/kg, while inspiratory and expiratory time was adjusted as required. Additionally, the fraction of inspired oxygen concentration (FiO_2) was set to 0.21 and all data from the ventilator and other measuring devices were recorded continuously for 3 min for each new ventilatory setting. Whenever SaO_2 dropped below 88 %, an open lung recruitment procedure was performed to improve oxygenation (Lachmann 1992; Spieth et al. 2011; Haitsma et al. 2003; Pomprapa et al. 2011) by introducing a higher peak inspiratory pressure (PIP) of 45 mbar for 3 breaths. The recovery of SaO_2 should generally take around 10 s after the recruitment maneuvers. Further investigation of CO_2 elimination can thereafter be performed.

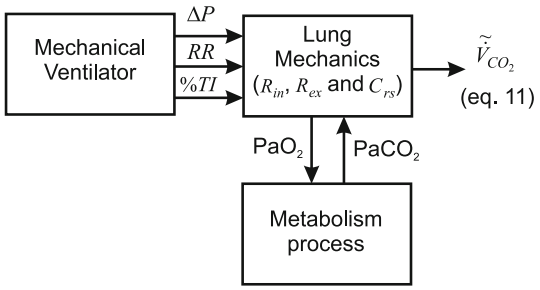

Fig. 5 A physical interpretation of a nonlinear relationship of CO_2 elimination based on Eq. (11)

Results

Tidal volume model

A simulation was performed to generate a contour of tidal volume based on adjustment of the temporal settings, e.g., RR and %TI. Tidal volume is a major factor for estimation of CO_2 elimination, as shown in Eq. (11). Its mathematical model is given in Eq. (7) and the simulation of tidal volume is shown in Fig. 6, based on the estimated parameters of lung mechanics in a healthy pig. The details of these estimated parameters of lung mechanics are given in the "Appendix II", which are derived by parameter identification using a least squares algorithm.

The contour of the tidal volume (Fig. 6) is plotted based on the assumption that all parameters of lung mechanics are constant. The simulation shows that tidal volume

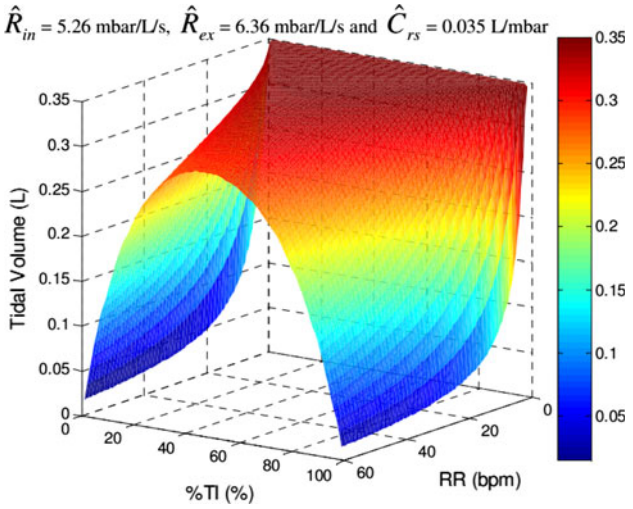

Fig. 6 Tidal volume contour with PIP = 10 mbar and PEEP = 0 mbar

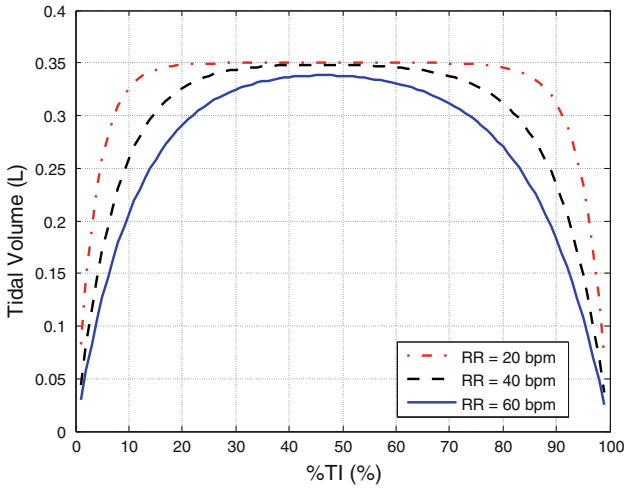

Fig. 7 The effect of %TI on tidal volume

gradually reduces when RR is increased for a %TI between 20 and 80 %. When considering %TI to be $\leq$ 20 % or $\geq$ 80 %, tidal volume is considerably decreased when RR is increased.

To see the effect of %TI on tidal volume provided in Fig. 7, we fix RR by cutting the contour with a plane, e.g., 40 bpm; tidal volume is then changed according to %TI in an inverted U-shape. The optimal tidal volume deviates slightly from the center of 50 % and, in this case, is positioned at %TI of 46.5 %.

An imbalanced inverted U-shape is caused by the difference between R_{in} and R_{ex}. If R_{in} is equivalent to R_{ex}, the optimal tidal volume will be on the adjustment of %TI at 50 %. Otherwise, the optimal tidal volume will be shifted from the center at 50 %. If R_{in} is $\leq R_{ex}$, the optimal tidal volume is positioned at a specific point with %TI $\leq$ 50 % and vice versa. A change in C_{rs} value causes a change in the size and shape of the contour.

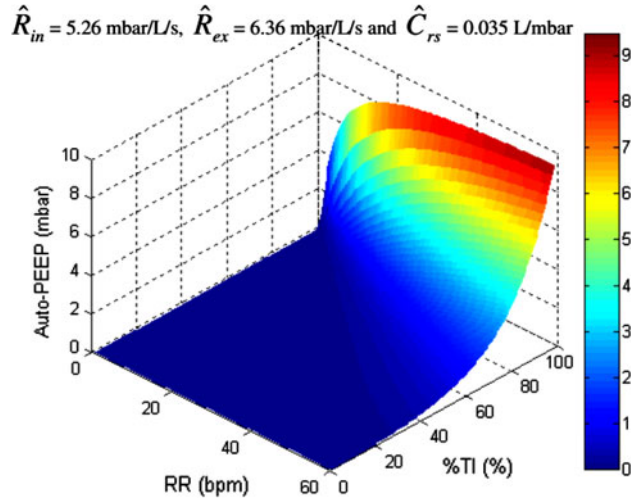

Fig. 8 Contour of autoPEEP with PIP = 10 mbar and PEEP = 0 mbar

AutoPEEP model

Insufficient expiratory time results in autoPEEP, or intrinsic PEEP. Its mathematical model is derived in Eq. (15) from the "Appendix I" and is shown in Fig. 8, based on parameters from a healthy pig. The existence of autoPEEP can be observed by a certain value of flow in the flow–time curve at the end of expiration. This simply means that there is a certain volume left in the lung at end-expiration. In the presence of autoPEEP, the lung cannot deflate to its normal volume influenced by PEEP, and additional volume provided in Eq. (14) is added on top of the FRC. Figure 8 shows that autoPEEP is dramatically increased with adjustment to a higher value of RR and a higher value of %TI. With a higher value of autoPEEP, less pressure difference is available for air ventilation and this causes a reduction in tidal volume (see Fig. 6).

Model of CO_2 elimination

Let us assume that the percentage of alveolar CO_2 concentration is constant at 4 % during an expiration. Under this assumption, Fig. 9 shows a theoretical contour of CO_2 elimination based on the parameters of a healthy pig. CO_2 elimination is a nonlinear response that relies on the temporal settings (RR and %TI) and driving pressure (ΔP). The shape and size of the response depend on ventilation settings, Eqs. (7) and (11), the subjects metabolism, and the properties of airway resistance and lung compliance.

Another simulation result of CO_2 elimination is shown in Fig. 10, based on the parameters of the lavaged pig serving as a model for ARDS with the following ventilation settings: FiO_2 = 0.21, RR = 30 bpm and %TI = 50 %. Compliance shows a significant decrease from 0.035 to 0.012 L/mbar due to loss of surfactant during lung lavage.

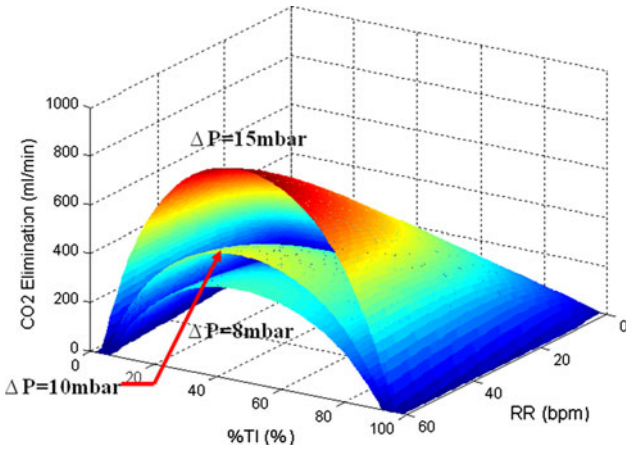

Fig. 9 Contour of CO_2 elimination with PEEP = 0 mbar, R_{in} = 5.26 mbar/L/s, R_{ex} = 6.36 mbar/L/s, C_{rs} = 0.035 L/mbar and $[etCO_2]$ = 4 %

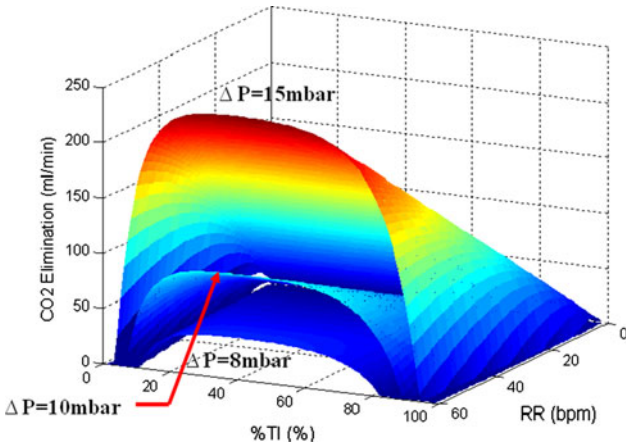

Fig. 10 Contour of CO_2 elimination from a lavaged pig with PEEP = 10 mbar, R_{in} = 4.75 mbar/L/s, R_{ex} = 8.15 mbar/L/s, C_{rs} = 0.012 L/mbar and $[etCO_2]$ = 4 %

The result shows a shape similar to that associated with parameters in a healthy condition, but a lower amount of CO_2 elimination. By fixing RR to a certain value, the optimal CO_2 elimination is shifted from %TI at 46.5 % (healthy condition) to %TI at 39 % (ARDS condition) due to the change of airway resistance.

Under this severe condition, the contour of Fig. 10 shows a considerable reduction in size compared with that in Fig. 9. The driving pressure (ΔP) has a considerable influence on tidal volume. With a higher driving pressure, more tidal volume can be achieved and this leads to more CO_2 volume during expiration. In contrast, ventilating with less driving pressure leads to less tidal volume and less CO_2 elimination. The effects of different driving pressures applied to a subject are presented in Figs. 9 and 10.

Model validation

Differences between measured CO_2 elimination ($\dot{V}_{CO_2}$) from Eq. (1) and estimated CO_2 elimination ($\tilde{\dot{V}}_{CO_2}$) from Eq. (11) are presented in Table 1. Based on the experiments, the mathematical model of CO_2 elimination was valid within some level of tolerance (on average 4.9 %). Therefore, the model can be used as a guideline to adjust ventilation settings e.g., PEEP, PIP, RR and %TI in order to control and optimize CO_2 elimination of the subject. The extreme case of 25 % error for the lavaged pig (case #2 lavaged) was excluded from the analysis of error mean because CO_2 elimination was very low (8 ml/min). In this case, the estimated CO_2 elimination was relatively accurate (6 ml/min). It is then biased to include this case for the analysis of model error.

Discussion

The main goal of the present work was to describe CO_2 elimination mathematically to increase understanding of the respiratory mechanism for CO_2 removal. Three parameters (ΔP, RR and %TI) from the ventilation settings are the major factors influencing CO_2 removal. Based on the mathematical model, CO_2 elimination is proportional to the driving pressure (ΔP). A higher amplitude of driving pressure, or a deeper breath, yields more tidal volume allowing more CO_2 to be removed from the lung. This applies particularly to the sick lung; however, considerable mechanical stress may be exerted on lung tissue which may contribute to the development of ventilator-induced lung injury. RR and %TI are two independent temporal settings of ventilation; they introduce a nonlinear effect on CO_2 elimination. Increasing RR with an optimal %TI setting is an alternative to increase CO_2 elimination, which is analytically proven and presented in Figs. 9 and 10. Additionally, an optimal value of %TI can be derived based on the imbalance of R_{in} and R_{ex}. Based on the parameter estimation, the optimal %TI should be tuned at around 40 % for maximal CO_2 removal (almost the physiological ratio of inspiration/expiration).

An incomplete expiration results in autoPEEP. This underlying pressure causes additional volume at the end of expiration. Tidal volume is technically reduced by the presence of autoPEEP. From Eq. (15), autoPEEP is a nonlinear function of driving pressure (ΔP), airway resistance, lung compliance, RR and %TI. A higher value of autoPEEP can be obtained by increasing driving pressure and setting a higher RR with higher %TI. However, applying autoPEEP is as controversial as the use of a high static PEEP. The adverse effects of autoPEEP include

Table 1 Model validation of CO_2 elimination from animal experiments 1 min after the change of ventilation variables

Animal	PEEP (mbar)	PIP (mbar)	RR (bpm)	%TI (%)	V_T (ml)	$\tilde{V}_D$ (ml)	[$etCO_2$] (%)	$\tilde{\dot{V}}_{CO_2}$ (ml/min)	$\dot{V}_{CO_2}$ (ml/min)	Error (%)
#1	0	10	27.3	50	250	86	3.28	147	150	−2
Healthy	0	10	60	70	149.2	65	3.78	191	207	−8.4
	0	18	27.3	86.3	247.1	73	3.13	148.8	155	−4
	5	11	27.3	50	141.5	73	4.21	78.7	73	7.8
	4	10	60	50	127.2	79	3.88	112	106	5.7
#2	0	10	20	50	339.2	85	3.85	195.7	196	−0.001
Healthy	0	10	40	46.6	300	93	3.24	268	257	4
	0	10	60	50	238	88	3.5	315	294	7
	5	12	20	16.7	201	91	4.8	105.6	99	6.7
	10	20	30	50	288	93	3.44	201	196	2.5
#2	5	18	20	50	298	89	3.55	148	139	6.5
Lavaged	4	18	20	50	315	91	3.55	159	150	6
	3	18	20	50	333	92	3.43	165	164	0.001
	9	21	40	80	89	34	0.27	6	8	−25
	9	21	40	46.7	259	94	3.26	215	234	−8.1

hemodynamic interference and risk of barotrauma due to air trapping in volume-controlled ventilation. However, the advantage of autoPEEP includes improvement of oxygenation and recruitment of collapsed alveoli (Kuckelt et al. 1981). More studies are required on the effects of autoPEEP on CO_2 elimination in patients with ARDS.

In our analysis, airway dead space is estimated based on the principle of the fraction of efficiency, obtained from the volumetric capnogram. From our estimation in Table 1, airway dead space (V_D) is a time-varying parameter and V_D/V_T lies between 0.25 and 0.6. Based on a CO_2 elimination model, airway dead space may be estimated using Eq. (11) with the measurement of breath-to-breath CO_2 elimination, $etCO_2$, RR and tidal volume. This approach provides an alternative assessment of airway dead space.

With resetting of the ventilator, CO_2 elimination changes immediately. Our mathematical model describes CO_2 elimination on a breath-by-breath basis. The change of CO_2 elimination correlates with the CO_2 partial pressure in arterial blood ($PaCO_2$) for homogeneous lungs (Kron et al. 1999). Naturally, whenever CO_2 elimination is not equal to CO_2 production, arterial CO_2 tension ($PaCO_2$) in the blood stream is either ascending or descending. To balance CO_2 elimination and CO_2 production, a standard blood gas analyzer should be used to evaluate $PaCO_2$ for a mechanically ventilated patient. The goal should, therefore, be a regulation of $PaCO_2$ at a specific value by adjusting ventilation parameters based on our proposed mathematical model.

However, it should be emphasized that in the present study the amount of CO_2 from blood was assumed to have an abundant supply from metabolism. In other words, there was no limitation to gas exchange on the alveolar surface. Thus, a more realistic contour of CO_2 elimination could be achieved if we add a constraint of limited space of lung volume, which (for simplification purposes) was not considered in the present analysis. However, the expected result will be the limitation of CO_2 elimination that should not exceed a certain value because of the restricted alveolar surface. Another limitation of our work is that we assumed a linear single compartment for lung mechanics. While this may be true for healthy lungs, the accuracy of CO_2 elimination model may be improved for diseased lungs using multi-compartment models and adding nonlinear flow–pressure relationships as in Rohrer's model (Crooke et al. 2003). In addition, due to the time-varying system, certain parameters such as compliance, inspiratory and expiratory resistances and others may not be constant during ventilation therapy. Our model is, therefore, less accurate in the sick lung than in a homogeneous healthy lung.

Conclusions

A mathematical model of CO_2 elimination was developed based on the principle of alveolar ventilation and of airway dead space estimation using a single-compartment model. It is shown that CO_2 elimination is a nonlinear function of multivariate parameters in terms of respiratory rate, percent inspiratory time, airway resistance, lung compliance, airway dead space, driving pressure, and percentage of end-tidal CO_2 concentration. The analytical solution provides insight into CO_2 elimination, which relies mainly on ventilation settings, lung mechanics and the patients

metabolism. In applying this model, not only can the driving pressure and respiratory rate be set higher to improve CO_2 elimination in ARDS patients, but airway resistance during inspiration and expiration should also be measured to determine the optimal %TI to maximize CO_2 elimination for treating patients with hypercapnia. Due to the low number of animals used for validation, the model cannot yet be generalized and requires further validation prior to clinical use.

Acknowledgments The authors thank Pulsion Medical Systems AG for their support, and Mr. Henrik Steinkraus for clinical assistance during the animal experiment at Charité University Hospital Berlin.

Appendix I: A mathematical derivation of tidal volume

Presented here is the mathematical proof of estimated tidal volume based on Eqs. (3) and (4). For inspiration, inspired tidal volume can be solved as simply an upwards exponential response given in Eq. (12).

$$V_i^{\mathrm{T}}(t) = (C_{\mathrm{rs}} \times \Delta P - V_{\mathrm{ex}}) \times (1 - e^{\frac{-t}{R_{\mathrm{in}} C_{\mathrm{rs}}}}) \tag{12}$$

Note that $V_i(t) = \mathrm{FRC} + V_{\mathrm{ex}} + V_i^{\mathrm{T}}(t)$

An expiration begins passively with an initial volume of $V_{\mathrm{T}} + V_{\mathrm{ex}}$. Thus, the exhaled tidal volume is governed by an exponential decay function as provided in Eq. (13).

$$V_e^{\mathrm{T}}(t) = (V_{\mathrm{T}} + V_{\mathrm{ex}}) \times e^{\frac{-t}{R_{\mathrm{ex}} C_{\mathrm{rs}}}} \tag{13}$$

Note that $V_e(t) = \mathrm{FRC} + V_{\mathrm{ex}} + V_{\mathrm{e}}^T(t)$

The final condition at the end-expiration is $V_{\mathrm{e}}^T(T_{ex}) = V_{\mathrm{ex}}$. From Eq. (13), with $T_{\mathrm{ex}} = \frac{60}{\mathrm{RR}} \times \left(1 - \frac{\%\mathrm{TI}}{100}\right)$, V_{ex} is given by

$$V_{\mathrm{ex}} = V_{\mathrm{T}} \times \frac{e^{\frac{-60 \times (1 - \%\mathrm{TI}/100)}{R_{\mathrm{ex}} C_{\mathrm{rs}} \times \mathrm{RR}}}}{\left(1 - e^{\frac{-60 \times (1 - \%\mathrm{TI}/100)}{R_{\mathrm{ex}} C_{\mathrm{rs}} \times \mathrm{RR}}}\right)}. \tag{14}$$

From Eq. (14), autoPEEP can be calculated by dividing $V_{\mathrm{ex}}(T_{\mathrm{ex}})$ by C_{rs} as shown in Eq. (15). In pressure-controlled mode, autoPEEP can be introduced to the subject by a minimization of T_{ex} or the increment of temporal settings (RR and %TI).

$$\mathrm{autoPEEP} = \frac{V_{\mathrm{T}}}{C_{\mathrm{rs}}} \times \frac{e^{\frac{-60 \times (1 - \%\mathrm{TI}/100)}{R_{\mathrm{ex}} C_{\mathrm{rs}} \times \mathrm{RR}}}}{\left(1 - e^{\frac{-60 \times (1 - \%\mathrm{TI}/100)}{R_{\mathrm{ex}} C_{\mathrm{rs}} \times \mathrm{RR}}}\right)} \tag{15}$$

From Eq. (12), the final condition at the end of tidal inspiration is $V_i^T(T_{in}) = V_T$ and tidal volume can be rearranged with a replacement of $T_{\mathrm{in}} = 60 \times \%\mathrm{TI}/(100 \times \mathrm{RR})$.

$$(C_{\mathrm{rs}} \Delta P - V_{\mathrm{ex}}) \times (1 - e^{\frac{-60 \times \%\mathrm{TI}/100}{R_{\mathrm{in}} C_{\mathrm{rs}} \times \mathrm{RR}}}) = V_{\mathrm{T}}.$$

Substituting Eq. (14) into the above equation and rearranging it, tidal volume can be solved as provided in Eq. (7), which is a nonlinear function of the ventilation settings and parameters of lung mechanics.

Appendix II: Parameter estimation of global lung mechanics

Based on measurement of ventilation obtained from the pigs shown in Fig. 11, for instance airway pressure (p_{aw}), flow ($\dot{V}$) and tidal volume (V), the parameters of lung mechanics ($\hat{R}_{\mathrm{in}}, \hat{R}_{\mathrm{ex}}$ and $\hat{C}_{\mathrm{rs}}$) can be identified by Eqs. (3) and (4) for the first half of the breathing cycle during inspiration and for the second half during expiration. This can be rewritten in terms of vector form with sampling time T_{s}, for instance during inspiration in Eq. (16).

$$\vec{p}_{\mathrm{aw}}(t) = \Theta \times \varphi + \vec{e}(t) \tag{16}$$

where $\vec{p}_{\mathrm{aw}}(t) = [p_{\mathrm{aw}}(0) \quad p_{\mathrm{aw}}(T_{\mathrm{s}}) \quad \ldots \quad p_{\mathrm{aw}}(T_{\mathrm{in}})]^T$, $\Theta = \begin{bmatrix} \dot{V}(0) & V(0) & 1 \\ \dot{V}(T_{\mathrm{s}}) & V(T_{\mathrm{s}}) & 1 \\ \dot{V}(2T_{\mathrm{s}}) & V(2T_{\mathrm{s}}) & 1 \\ \vdots & \vdots & \vdots \\ \dot{V}(T_{\mathrm{in}}) & V(T_{\mathrm{in}}) & 1 \end{bmatrix}$ $\varphi = \begin{bmatrix} \hat{R}_{\mathrm{in}} \\ \frac{1}{\hat{C}_{\mathrm{rs}}} \\ \mathrm{autoPEEP} \end{bmatrix}$ and $\vec{e}(t)$ is an error vector.

The parameters $\hat{R}_{\mathrm{ex}}$ and $\frac{1}{\hat{C}_{\mathrm{rs}}}$ can be computed using least-squares estimation provided in Eq. (17), derived by the minimization of the squared error function (Ljung 1999).

$$\hat{\varphi} = (\Theta^T \times \Theta)^{-1} \times \Theta^T \times \vec{p}_{\mathrm{aw}}(t) \tag{17}$$

Similarly, $\hat{R}_{\mathrm{in}}$ can be estimated using Eq. (16) by replacing the ventilation measurements in the other half of breathing cycle from the beginning of expiration to the end of expiration. Regarding the data set in Fig. 11, all parameters

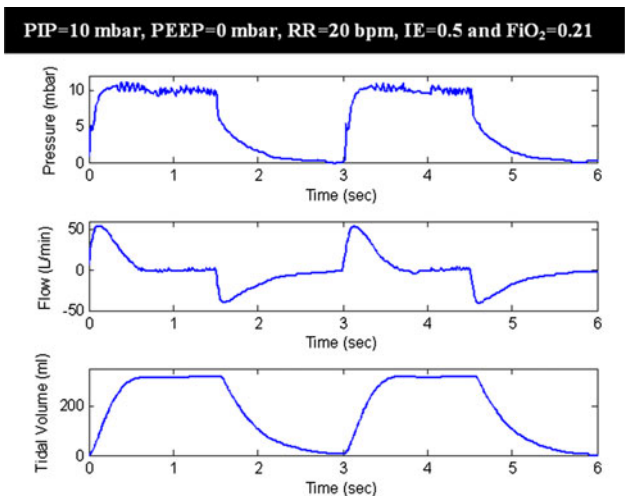

Fig. 11 Ventilatory data for parameter estimation from a healthy pig

of lung mechanics can be obtained: $\hat{R}_{in}$ = 5.26 mbar/L/s, $\hat{R}_{ex}$ = 6.36 mbar/L/s and $\hat{C}_{rs}$ = 0.035 L/mbar. Inspiratory time constant ($\tau_{in} = \hat{R}_{in} \times \hat{C}_{rs}$) is about 0.18 sec and expiratory time constant ($\tau_{ex} = \hat{R}_{ex} \times \hat{C}_{rs}$) is 0.22 s. Note that all these parameters were identified from a healthy pig. Likewise, the parameter estimation of lavaged condition can be obtained using the same algorithm for the ventilatory data from a lavaged pig.

References

Aboab J, Niklason L, Uttman L, Brochard L, Jonson B (2012) Dead space and CO_2 elimination related to pattern of inspiratory gas delivery in ARDS patients. Crit Care 16(2):R39

Amato MB, Barbas CS, Medeiros DM, Magaldi RB, Schettino GP, Lorenzi-Filho G, Kairalla RA, Deheinzelin D, Munoz C, Oliveira R, Takagaki TY, Carvalho CR (1998) Effect of a protective ventilation strategy on mortality in the acute respiratory distress syndrome. New Engl J Med 338:347–354

Ashbaugh DG, Bigelow DB, Petty TL, Levine BE (1967) Acute respiratory distress in adults. Lancet 290:319–323

Bauer CR (1982) Does carbon dioxide play a role in retrolental fibroplasia? Pediatries 70:663

Beitler JR, Hubmayr RD, Malhotra A (2013) CrossTalk opposing view: there is not added benefit to providing permissive hypercapnia in the treatment of ARDS. J Physiol 591(Pt 11):2767–2769

Breen PH, Isserles SA, Harrison BA, Roizen MF (1992) Simple computer measurement of pulmonary VCO_2 per breath. J Appl Physiol 72(5):2029–2035

Breen PH, Mazumdar B. (1996) How does positive end-expiratory pressure decrease VCO_2 elimination from the lung? Respir Physiol. 103(3):233–242

Crooke PS, Hota S, Marini JJ, Hotchkiss JR (2003) Mathematical models of passive, pressure-controlled ventilation with different resistance assumptions. Math Models Passiv Press Control Vent Differ Resist Assumpt 38:495–502

Devaquet J, Jonson B, Niklason L, Si Larbi A-G, Uttmann L, Aboab J, Brochard L (2008) Effects of inspiratory pause on CO_2 elimination and arterial PCO_2 in acute lung injury. J Appl Physiol 105:1944–1949

Dorrington KL, Talbot NP (2004) Human pulmonary vascular responses to hypoxia and hypercapnia. Pflugers Arch 449(1):1–15

Fletcher R, Jonson B, Cumming G and Brew J (1981) The concept of deadspace with special reference to the single breath test for carbon dioxide. Br J Anaesth 53:77–88

Fletcher R, Jonson B (1984) Deadspace and the single breath test for carbon dioxide during anaesthesia and artificial ventilation. Br J Anaesth 56:109–119

Fletcher R. On-line expiratory CO_2 monitoring. Int J Clin Monit Comput (1986) 3(3):155–163

Girard TD, Bernard GR (2007) Mechanical ventilation in ARDS: a state-of-the-art review. Chest 131:921–929

Haitsma JJ, Lachmann R, Lachmann B (2003) Open lung in ARDS. Acta Phamacol Sin 12:1304–1307

Hickling KG, Joyce C (1995) Permissive hypercapnia in ARDS and its effect on tissue oxygenation. Acta Anaesthesiol Scand Suppl 107:201–208

Krishnan JA and Brower RG (2000) High-frequency ventilation for acute lung injury and ARDS. Chest 118(3):795–807

Kron A, Boehm S, Leonhardt S (1999) An analytic model for the CO_2 mass balance in mechanically ventilated patients. European medical and biomedical engineering conference. Vienna (Austria), November 1999

Kuckelt W, Scharfenberg J, Mrochen H, Dauberschmidt IR, Petrakov G, Kassil W and Meyer M (1981) Effect of PEEP on gas exchange, pulmonary mechanics, and hemodynamics in adult respiratory distress syndrome (ARDS) Intensive Care Med 7:177–185

Lachmann B, Robertson B, and Vogel J (1980) In vivo lung lavage as an experimental model of the respiratory distress syndrome. Acta Anaesthesiol Scand 24:231–236

Lachmann B, Schairer W, Armbruster S, van Daal GJ, Erdmann W (1989) Improved arterial oxygenation and CO_2 elimination following changes from volume-generated PEEP ventilation with inspiratory/expiratory (I:E) ratio of 1:2 to pressure-generated ventiatlion with I/E ratio of 4:1 in patients with severe adult respiratory distress syndrome (ARDS). Adv Exp Med Biol 248:779–786

Lachmann B (1992) Open up the lung and keep it open. Intensive Care Med 18:319–321

Larsson A (1992) Elimination of apparatus dead space a simple method for improving CO_2 removal without increasing airway pressure. Acta Anaesthesiol Scand 36(8):796–799

Leonhardt S, Boehm S and Lachmann B (1998) Optimierung der Beatmung beim akuten Lungenversagen durch Identifikation physiologischer Kenngroessen. Automatisierungstechnik 46:532–539

Lindahl SGE, Offord KP, Johannesson GP, Meyer DM, Hatch DJ (1989) Carbon dioxide elimination in anaesthetized children. Can J Anaesth 36(2):113–119

Lipsky JA, Angelone A (1967) Breath-by-breath CO_2 elimination by analog computer techniques. Med Res Eng 6(3):11–15

Ljung L (1999) System identification theory for the user. Prentice Hall, New Jersy, pp 545

Marx P, Weinert G, Pfiester P, Kuhn H (1973) The influence of hypercapnia and hypoxia on intracranial pressure and on CSF electrolyte concentrations. Adv Neurosurg 1:195–198

Marini JJ, Crooke III PS, Truwit JD (1989) Determinants and limits of pressure-preset ventilation: a mathematical model of pressure control. J Appl Physiol 67(3):1081–1092

Mekontso DA, Charron C, Devaquet J, Aboab J, Jardin F, Brochard L, Vieillard-Baron A (2009) Impact of acute hypercapnia and augmented positive end-expiratory pressure on right ventricle function in severe acute respiratory distress syndrome. Intensive Care Med 35(11):1850–1858

Mughal MM, Culver DA, Minai OA and Arroliga AC (2005) Auto-positive end-expiratory pressure: mechanisms and treatment. Cleve Clin J Med 72(9):801–809

NHLBI (2000) Ventilation with lower tidal volumes as compared with traditional tidal volumes for acute lung injury and the acute respiratory. New Engl J Med 342:1301–1308

Pomprapa A, Schwaiberger D, Lachmann B, Leonhardt S (2011) Computation and monitoring CO_2 elimination for 'Open Lung' recruitment. Eur Soc Comput Technol Anaesth Intensive Care. 26–27

Saidel GM, Chang YA (1994) CO_2 control of breathing: parameter estimation and stability evaluation. Med Eng Phys 16:135–142

Sinha P, Flower O, Soni N (2011) Deadspace ventilation: a waste of breath! Intensive Care Med 37:735–746

Slutsky AS, Kamm RD, Rossing TH, Loring SH (1981) Effects of frequency, tidal volume, and lung volume on CO_2 elimination in dogs by high frequency (2–30 Hz), low tidal volume ventilation. J Clin Invest 68:1475–1484

Spieth PM, Gldner A, Carvalho AR, Kasper M, Pelosi P, Uhlig S, Koch T, Gama de Abreu M (2011) Open lung approach vs acute

respiratory distress syndrome network ventilation in experimental acute lung injury. Br J Anaesth 107(3):388–397

Taskar V, John J, Larsson A, Wetterberg T, Jonson B (1995) Dynamics of carbon dioxide elimination following ventilator resetting. Chest 108:196–202

Thorens JB, Jolliet P, Ritz M, Chevrolet JC (1996) Effects of rapid permissive hypercapnia on hemodynamics, gas exchange, and oxygen transport and consumption during mechanical ventilation for the acute respiratory distress syndrome. Intensive Care Med 22(3):182–191

Tusman G, Bohm SH, Suarez-Sipmann F, Scandurra A, Hedenstierna G (2010) Lung recruitment and positive end-expiratory pressure have different effects on CO_2 elimination in healthy and sick lungs. Anesth Analg 111:968–977

Webster JG (2009) Medical instrumentation application and design. Wiley, New Jersy, pp 396